



10-2022

(SI10-068) Performance Analysis of Cosine Window Function

Vikas Misra
Jaypee University of Engineering and Technology

Narendra Singh
Jaypee University of Engineering and Technology

M. Shukla
Rajkiya Engineering College

Follow this and additional works at: <https://digitalcommons.pvamu.edu/aam>



Part of the [Harmonic Analysis and Representation Commons](#)

Recommended Citation

Misra, Vikas; Singh, Narendra; and Shukla, M. (2022). (SI10-068) Performance Analysis of Cosine Window Function, *Applications and Applied Mathematics: An International Journal (AAM)*, Vol. 17, Iss. 3, Article 9. Available at: <https://digitalcommons.pvamu.edu/aam/vol17/iss3/9>

This Article is brought to you for free and open access by Digital Commons @PVAMU. It has been accepted for inclusion in *Applications and Applied Mathematics: An International Journal (AAM)* by an authorized editor of Digital Commons @PVAMU. For more information, please contact hvkoshy@pvamu.edu.



Performance Analysis of Cosine Window Function

^{1*}Vikas Misra, ²Narendra Singh, and ³M. Shukla

^{1,2}Department of Electronics & Communication Engineering
Jaypee University of Engineering and Technology
A-B Road, Raghogarh, Guna-473226 (MP), India

³Rajkiya Engineering College
Kannauj-209732 (UP), India

^{1*}vikasalld@gmail.com; ²narendra.singh@juet.ac.in; ³manojkrshukla@gmail.com

*Corresponding Author

Received: November 20, 2021; Accepted: August 13, 2022

Abstract

This paper reviews the mathematical functions called the window functions which are employed in the Finite Impulse Response (FIR) filter design applications as well as spectral analysis for the detection of weak signals. The characteristic properties of the window functions are analyzed and parameters are compared among the known conventional cosine window (CW) functions (Rectangular, Hamming, Hanning, and Blackman) and the variable Kaiser window function. The window function expressed in the time domain can be transformed into the frequency domain by taking the Discrete Fourier Transform (DFT) of the time domain window function. The frequency response of the window function so obtained has main lobe, side lobes, and roll-off rate of side lobes. The main lobe width (MLW) expressed in 3dB bandwidth (BW), highest side lobe level (HSL), and side lobe roll-off rate (SLROR) of the conventional window function and variable Kaiser window is then evaluated from the frequency response and compared to find out the appropriate window for employed applications.

Keywords: DFT; FIR Filter; Cosine window function; Windowing; Main-lobe width; Side-lobe level; SLROR; Spectral analysis; Spectrum leakage; Gibb's phenomena

MSC 2010 No.: 42A05, 42A16, 42A38

1. Introduction

As widely known, Discrete Fourier Transform is used to decompose a time-domain signal into its frequency components. But limitations of DFT arise when practical signals having non-integer periods are considered, and the outcome produces sharp transitions or jump discontinuities. Thus, the output spectrum does not replicate the original signal but gets distorted. The distortions lead to spectrum leakage or smearing of the signal (Hamming (1976)). To mitigate the effect of discontinuity at the sharp edges, windowing is employed. These window functions are mathematical functions that are employed to smoothen the sharp transition or jump discontinuities. The well-known application of window functions is spectrum analysis for the detection of weaker signals among high-frequency components. Window functions have also strongly played a role in designing the FIR filters through a method popularly known as windowing. The most typical frequency-selective ideal filter is the conventional brick wall filter or rectangular filter. The infinite duration of the filter's ideal impulse response, if truncated by a window function, is realized by multiplying the infinite impulse response with the window function, one can get a smoother finite duration, realizable and linear phase FIR filters.

These window functions have gained a wide space in literature. Harris (1978) has reported a wide variety of window functions. Kaiser (1974) has devised an FIR filter with variable parameters. Kaiser window can be transformed closely to any of conventional CW functions by suitable choice of a variable parameter β . Spectrum analysis and estimation methods are presented in Geckinli (1974), Yoon and Joo (1974), and Zaytsev and Khzmalyan (1974). Various window functions have been utilized in designing prototype filter used in the construction of filter banks and transmultiplexers (Datar et al. (2010); Singh and Saxena (2012); Kumar et al. (2015); Ozdemir and Karaboga (2020); Avcı and Gümüşsoy (2020); Garg et al. (2013)). Recently many optimization techniques have been introduced in window-based filter design. Sharma et al. (2010) has utilized swarm optimization algorithms for window-based filter bank designs. A wide variety of applications of window functions have been discussed in Prabhu (2014).

The following section of this paper is categorized as follows. Section 2 describes the window characteristics and the steps for low pass FIR filter design along with the time-domain representation of the conventional window functions and variable Kaiser window. Section 3 presents the simulated results of the discussed windows along with their comparison, and lastly, Section 4 concludes the paper.

2. Window Characteristics

The conventional CW functions like Rectangular, Hamming, Hanning, and Blackman and variable Kaiser window can be differentiated with the following main characteristics of windows.

- There is one main lobe and multiple smaller side lobes in the continuous spectrum frequency response of the window as shown in Figure 1.
- The time domain signal may contain multiple frequency components, and hence at each fre-

quency component, the main lobe is centered around it, with the side lobe approaching zero.

- The side lobes control leakage, high side lobes mean high leakage, hence side lobes of large amplitude signal can shadow the main lobe of weak amplitude signal of nearby frequency.
- As the tapering or SLROR of the side lobe goes steeper, the spectrum leakage becomes weaker.
- The Main lobe controls resolution hence for sharper transitions, the main lobe should be narrower giving better frequency resolution.
- Lower side lobe levels are required for the perceptibility of weak tone signals among high amplitude strong signals.
- Slimmer main lobe and lower side lobes are contradictory to each other; hence a fair trade-off is required as per the required application of windows.

Thus, with the knowledge of the above characteristics, CW functions can be designed to achieve the desired results for the specific application.

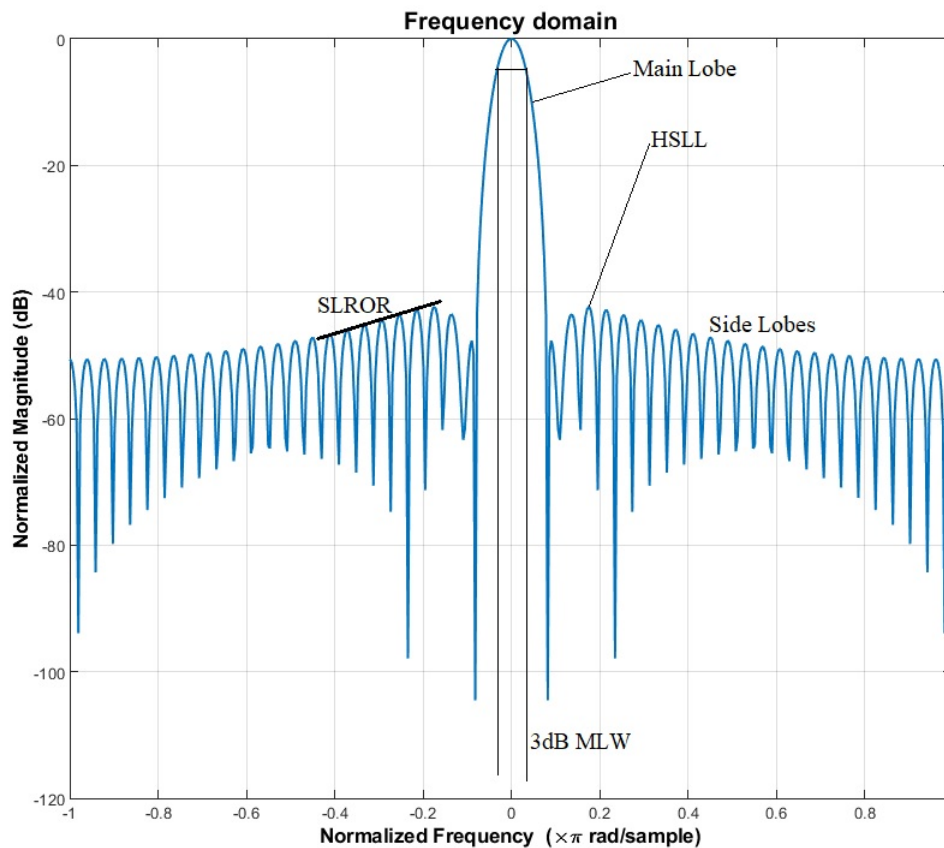


Figure 1. Plot of frequency domain representation of Hamming window illustrating the description of the characteristics Main Lobe, Side Lobes, HSSL, SLROR and 3dB MLW

2.1. Steps for low pass FIR filter design:

The frequency response of an ideal low pass filter (LPF) having central frequency ω_c is given as

$$H_{ideal}(\omega) = \begin{cases} 1, & |\omega| < \omega_c, \\ 0, & \omega_c < |\omega| < \pi. \end{cases} \quad (1)$$

Taking the inverse of DFT, the time domain equivalent of (1) is obtained as

$$h_{ideal}(n) = \frac{1}{2\pi} \int_{-\pi}^{+\pi} H_{ideal}(\omega) e^{j\omega n} d\omega. \quad (2)$$

Putting (1) in (2), we get

$$h_{ideal}(n) = \frac{1}{2\pi} \int_{-\omega_c}^{+\omega_c} e^{j\omega n} d\omega = \frac{\sin(\omega_c n)}{\pi n}. \quad (3)$$

Now the following steps are summarised to design low pass FIR filter by window method:

1. The frequency response of the filter is desired same as the frequency response of ideal LPF as obtained in (3) above, hence the desired impulse response, with center frequency ω_c , is given by

$$h_{lpf_d}(n) = \frac{\sin(\omega_c n)}{\pi n}, \quad \text{where } -\infty < n < \infty. \quad (4)$$

2. Since (4) ranges infinity, hence not realizable, therefore to make it causal and realizable, shifted impulse response is required as

$$h_{lpf_d}(n) = \frac{\sin(\omega_c(n - 0.5N))}{\pi(n - 0.5N)}, \quad \text{where } 0 < n < (N - 1), \quad (5)$$

where N is the rectangular window length. This direct truncation of impulse response causes the sizable amplitude ripples at both the sharp edges or discontinuities of the passband and stopband region, popularly known as Gibb's phenomena.

3. As a solution to reduce the unwanted ripples in both the edges, the window function $w(n)$ is applied to get the filter's impulse response $f(n)$, as defined in Singh and Saxena (2013), as

$$f(n) = h_{lpf_d}(n) \cdot w(n). \quad (6)$$

4. Calculate and realize the transfer function $F(z)$ by obtaining z -transform of $f(n)$ as given in Kumar et al. (2014).

$$F(z) = \sum_{n=0}^{N-1} f(n) z^{-n}. \quad (7)$$

2.2. Window functions in time domain and their time-frequency plot representation:

1. Rectangular window:

$$w(n) = \begin{cases} 1, & 0 \leq n \leq N - 1, \\ 0, & \text{otherwise.} \end{cases} \quad (8)$$

2. Hamming Window:

$$w(n) = \begin{cases} 0.54 - 0.46 \cos\left(\frac{2\pi n}{N-1}\right), & 0 \leq n \leq N - 1, \\ 0, & \text{otherwise.} \end{cases} \quad (9)$$

3. Hanning Window:

$$w(n) = \begin{cases} 0.5 - 0.5 \cos\left(\frac{2\pi n}{N-1}\right), & 0 \leq n \leq N - 1, \\ 0, & \text{otherwise.} \end{cases} \quad (10)$$

4. Blackman Window:

$$w(n) = \begin{cases} 0.42 - 0.5 \cos\left(\frac{2\pi n}{N-1}\right) + 0.08 \cos\left(\frac{4\pi n}{N-1}\right), & 0 \leq n \leq N - 1, \\ 0, & \text{otherwise.} \end{cases} \quad (11)$$

5. Kaiser Window:

$$w(n) = \begin{cases} \frac{I_0(\beta \sqrt{1 - (\frac{n-k}{k})^2})}{I_0(\beta)}, & 0 \leq n \leq N - 1, \\ 0, & \text{otherwise,} \end{cases} \quad (12)$$

where $k = (N - 1)/2$, and I_0 is a zeroth-order modified Bessel function of the first kind. β is the variable parameter of the Kaiser window function, which acts as a controlling factor between the width of the main lobe and the side lobe level.

In Figure 2 the time domain of the rectangular window has abrupt edges at the ends points. The curve in the time domain of Figures 4 and 5 rises from zero from the endpoints and reaches its peak in the center, and in Figure 3 it rises from the non-zero level. The frequency domains show the breadth of the central main lobe, the multiple small side lobes with the highest side lobe adjacent to the main lobe, except for the hamming window in Figure 3, where the HSSL is not the adjacent side lobe with the main lobe. The above-discussed CW functions can be closely derived from the Kaiser window, by suitably selecting the variable parameter β . Figure 6 represents Kaiser window with values $\beta = 2, 4.5$, and 7. It can be easily viewed that as β increases, it lowers the levels of side lobes, but at the cost of the increased width of the main lobe. Comparing the CW window

characteristics, it is easily verified that by carefully selecting the values of β , the Kaiser window can be nearly modified to the CW window. Thus, for $\beta = 0$, the Kaiser window is equivalent to rectangular, while for $\beta = 5, 6$, and 8.6 , the Kaiser window is close to the Hanning, Hamming, and Blackman window respectively as represented in Figure 7.

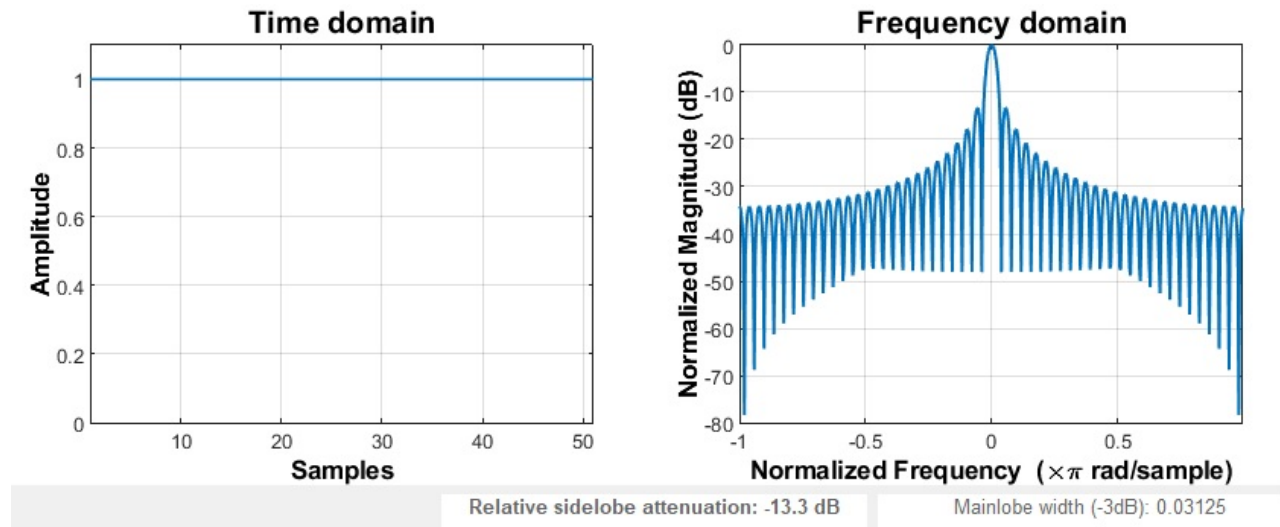


Figure 2. Time and frequency response of Rectangular window

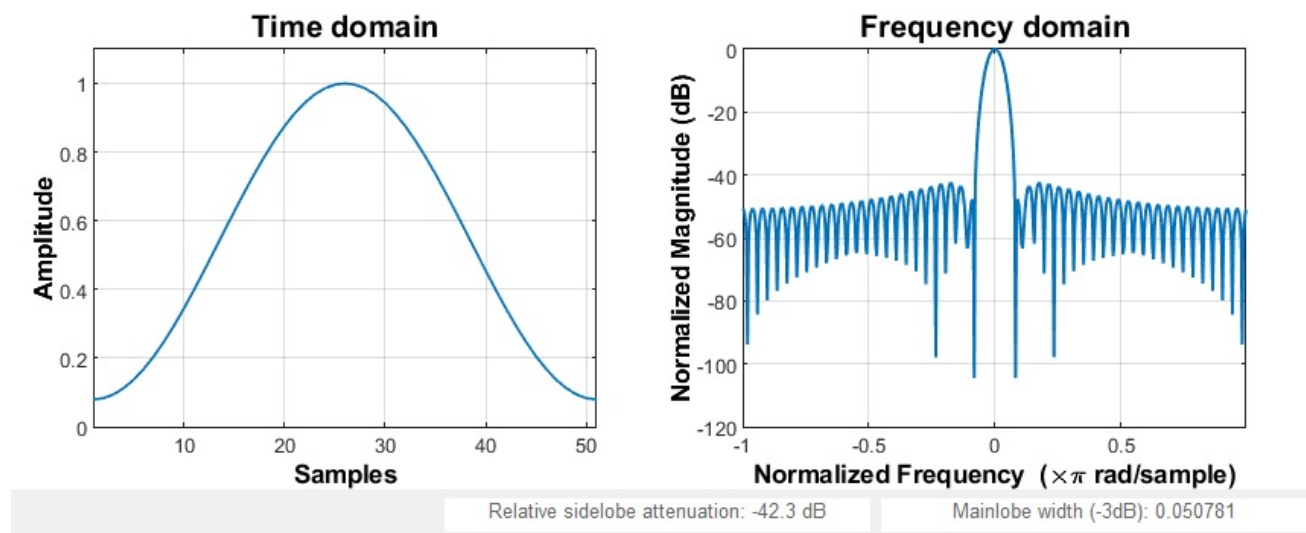


Figure 3. Time and frequency response of Hamming window

3. Simulation results and comparison

The conventional CW window function and its application in the design of low pass FIR filters have been simulated and their characteristic values are taken to compare the performance. The Length of windows simulated has been taken as ($L = 51$) and the central frequency of LPF designed by these windows has been taken as ($\omega_c = 0.1\pi$).

The simulation output of CW windows has been tabulated in Table 1 where MLW, HSSL and SLROR are the parameters of window functions. The corresponding time and frequency responses of these window functions presented in Figure 2 to Figure 7. Among conventional CW functions discussed, the Rectangular window has got least MLW and high sidelobes (HSSL = $-13.3dB$), and the Blackman window has got the high MLW but low HSSL of $-58dB$ as in Table 1. This is due to the additional cosine term in Blackman window in (11). It is also observed that high and desirable SLROR of $-18dB/octave$ is achieved by Hanning and Blackman window. In the adjustable Kaiser window as the value of variable parameter β increases, the MLW also increases, but the amplitude of the side lobes (HSSL) decreases. The values of parameters of conventional CW functions and Kaiser window function with the value of $\beta = 0, 5, 6,$ and 8.6 is evaluated and presented in Table 1.

Figure 8 (a), (b), (c), and (d) present the magnitude responses (normalized to 1) of the low pass FIR filter designed by rectangular, Hamming, Hanning, and Blackman windows respectively along with zoomed passband region having a centre frequency as $\omega_c = 0.1\pi$. The LPF designed by rectangular window shows large ripples in both passband and stopband region, but least transition width in Figure 8 (a). These ripples are due to large sidelobes present in the rectangular window function. The amplitude of ripples decreases from rectangular, Hamming, Hanning, and least in Blackman window but transition width increases accordingly as observed in Figures 8 (b),(c), and (d) respectively. The transition width of the filter depends directly on the MLW of the window used (Sharma et al. (2007)).

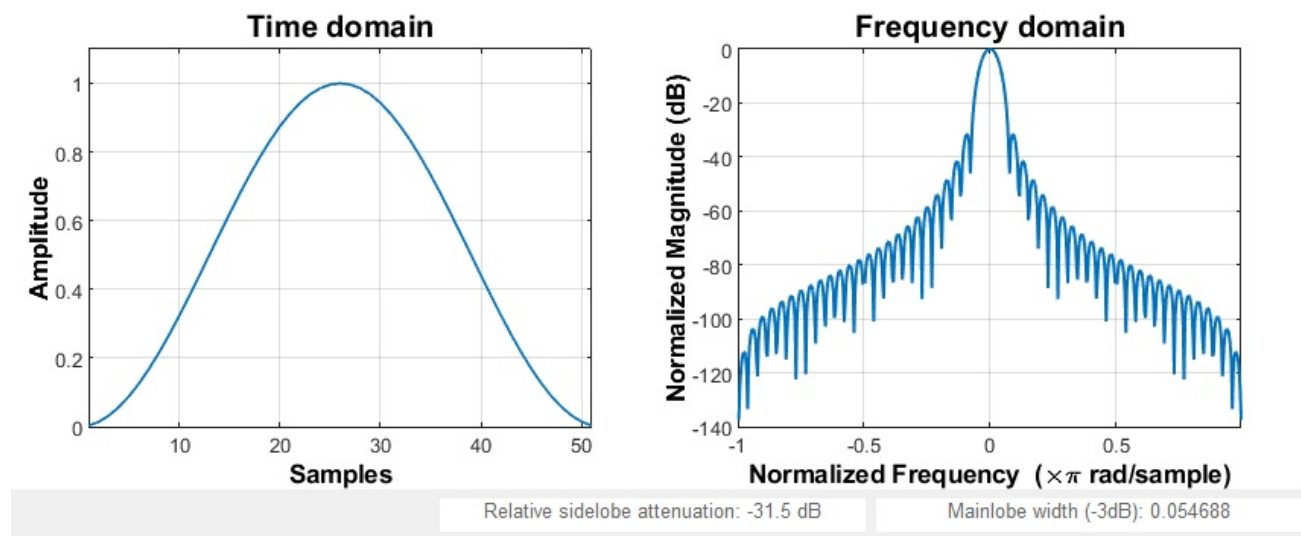


Figure 4. Time and frequency response of Hanning window

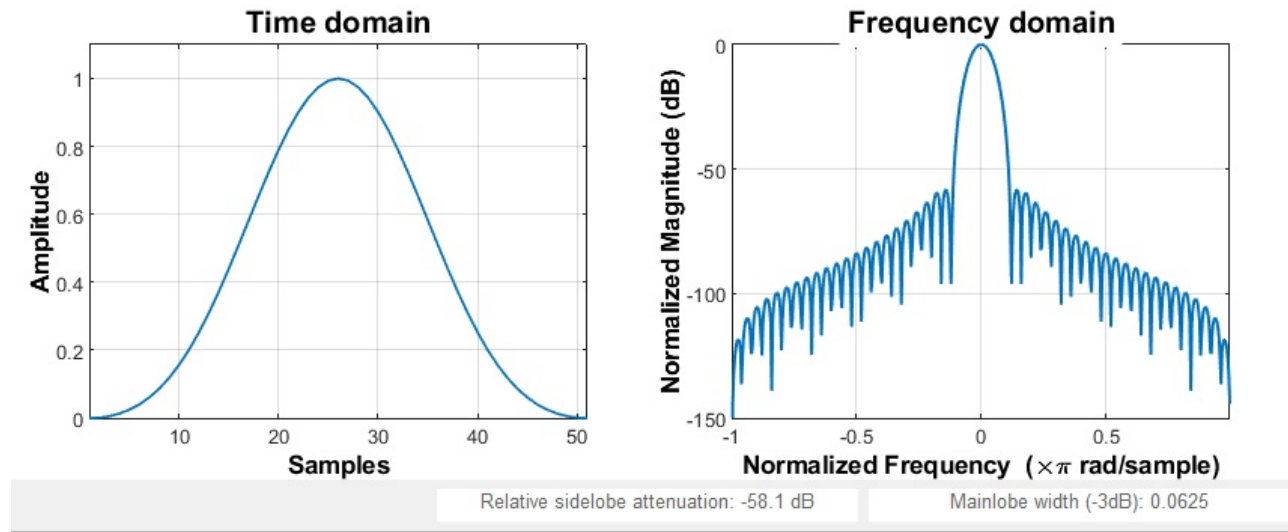


Figure 5. Time and frequency response of Blackman window

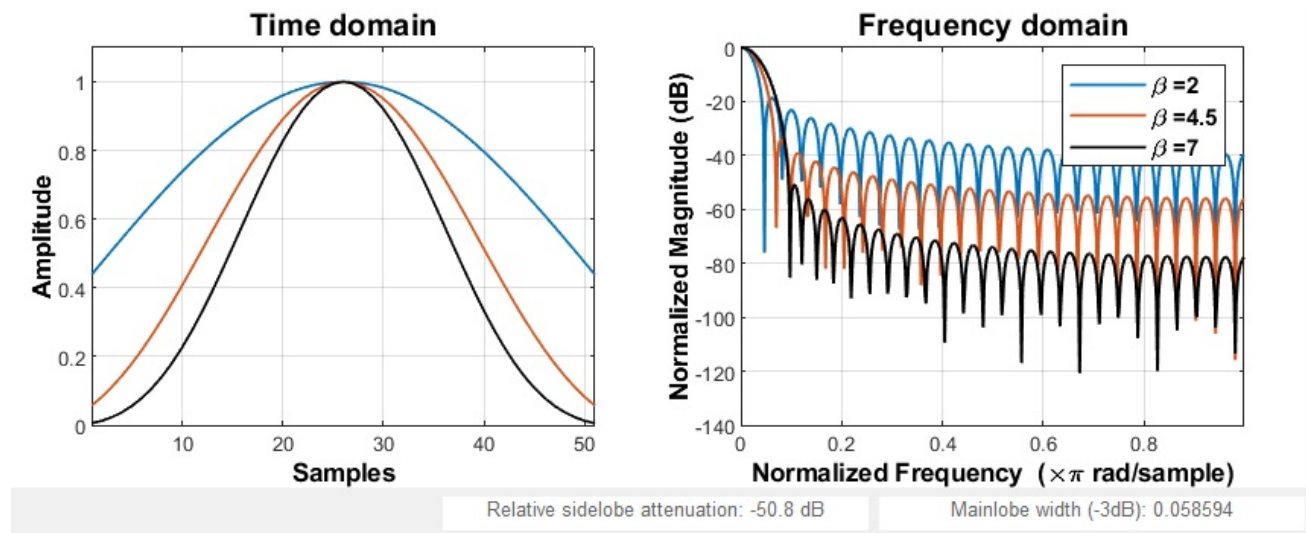


Figure 6. Time and frequency response of Kaiser window for values of $\beta=2, 4.5$ and 7

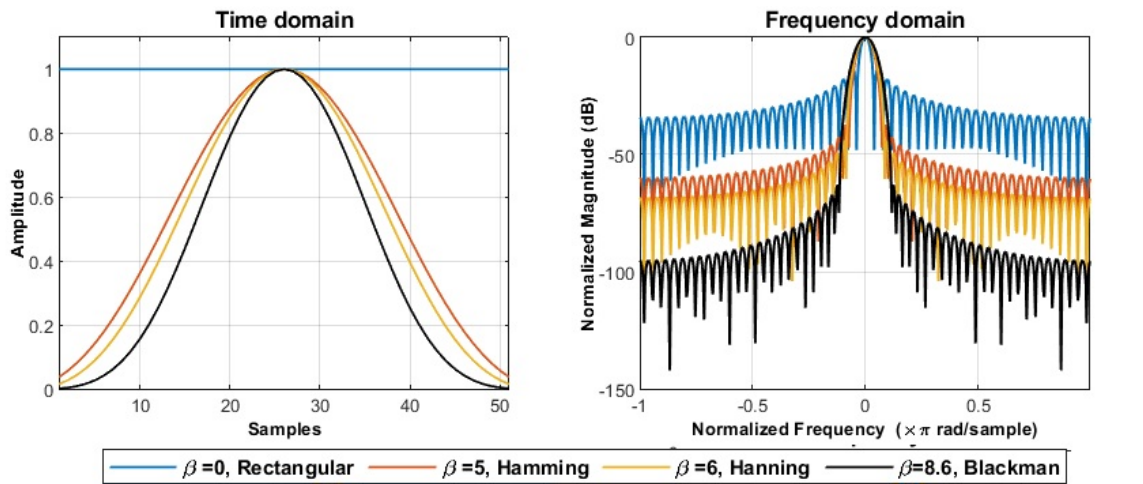


Figure 7. Kaiser window performs like CW functions for the value of $\beta=0$ (Identical to Rectangular window), $\beta=5$ (Close to Hamming window), $\beta=6$ (Close to Hanning window), and $\beta=8.6$ (Close to Blackman window), having discrete time length $N=51$

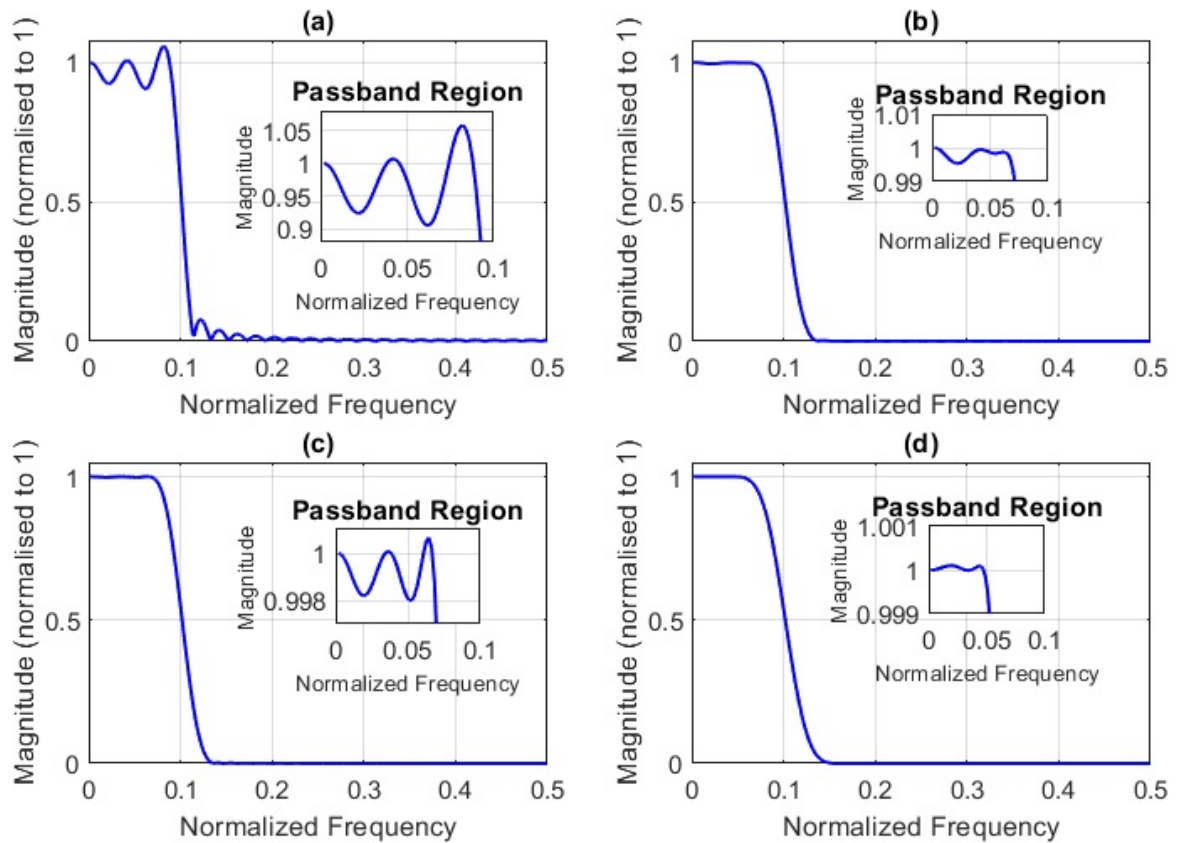


Figure 8. Magnitude Response of low pass FIR filter designed by (a) Rectangular, (b) Hamming, (c) Hanning, and (d) Blackman window along with zoomed passband region in plotted magnitude response of the filter. The centre frequency taken is $\omega_c = 0.1\pi$, to design the filter.

Table 1. Performance comparison of CW windows and Kaiser Window

Name of Window(N)	MLW(-3dB)	HSLL (in dB)	SLROR
Rectangular (51)	0.03125	-13.3	-6 dB/octave
Hamming (51)	0.050781	-42.3	-6 dB/octave
Hanning (51)	0.054688	-31.5	-18 dB/octave
Blackman (51)	0.0625	-58.1	-18 dB/octave
Kaiser (51,2)	0.039063	-18.7	-6 dB/octave
Kaiser (51,4.5)	0.046875	-34.1	-6 dB/octave
Kaiser (51,7)	0.058594	-50.8	-6 dB/octave
Kaiser (51,0)	0.03125	-13.3	-6 dB/octave
Kaiser (51,5)	0.050781	-37.4	-6 dB/octave
Kaiser (51,6)	0.054688	-44.0	-6 dB/octave
Kaiser (51,8.6)	0.0625	-62.7	-6 dB/octave

4. Conclusion

Windows are the tools to alleviate the artifacts of DFT of non-integer periodic signals. The simulation and analysis of the conventional CW function have been conducted in this paper, which has a simple design and expression while the Kaiser window being variable, can be closely modified to CW windows by carefully tuning the variable parameter. A comparison among various discussed windows is also presented showing the variation of main lobe width against the side lobe levels deviations along with low pass FIR filter designed with these windows possessing ripples in passband and stopband and variation of transition width of the filter according to the MLW of the window function. Although there is no common rule for selecting a window function, the best performer among many window functions is chosen as per the requirement of the application. Still, on the other side, the parameters tabulated might help in making the right choice.

Acknowledgment:

The authors are grateful to the Editor-in-Chief and anonymous reviewers for the careful reading, constructive comments and suggestions which permit us to improve the paper.

REFERENCES

- Avcı, K. and Gümüşsoy, E. (2020). Design, analysis, and ECG subband processing application of new M-channel cosine modulated uniform filter banks based on exponential window family, J. Fac. Eng. Archit. Gazi Univ. <https://doi.org/10.17341/gazimmfd.451652>
- Datar, A., Jain, A. and Sharma, P. (2010). Design of Kaiser window based optimized prototype

- filter for cosine modulated filter banks, *Signal Processing*, Vol. 90, No. 5, pp. 1742-1749. <https://doi.org/10.1016/j.sigpro.2009.11.011>
- Garg, A., Saxena, A., Arora, A. and Singh, N. (2013). Implementation of optimized transmultiplexer using combinational window functions, *International Journal of Advance Research*, Vol. 1, No. 8, pp. 1-5.
- Geckinli, N. (1983). Discrete Fourier transforms and its applications to power spectra estimation, *Signal Processing*, Vol. 5, No. 5, p. 469. [https://doi.org/10.1016/0165-1684\(83\)90011-7](https://doi.org/10.1016/0165-1684(83)90011-7)
- Hamming, R.W. (1989). *Digital Filters* (3rd ed.), Dover Publication, NY.
- Harris, F.J. (1978). On the use of windows for harmonic analysis with the Discrete Fourier Transform, *Proceedings of the IEEE*, Vol. 66, No. 1. <https://doi.org/10.1109/PROC.1978.10837>
- Kaiser, J.F. (1974). Nonrecursive digital filter design using the Io-sinh window function, *Proc. 1974 IEEE Int. Symp. Circuit Theory*, pp. 20–23.
- Kumar, A., Pooja, R. and Singh, G. (2014). Design and performance of closed form method for cosine modulated filter bank using different windows functions, *International Journal Of Speech Technology S*, Vol. 17, pp. 427-441. <https://doi.org/10.1007/s10772-014-9242-8>
- Kumar, A., Singh, G. and Anurag, S. (2015). An optimized cosine-modulated nonuniform filter bank design for subband coding of ECG signal, *Journal Of King Saud University - Engineering Sciences*, Vol. 27, No. 2, pp. 158-169. <https://doi.org/10.1016/j.jksues.2013.10.001>
- Ozdemir, G. and Karaboga, N. (2020). Uniform cosine modulated filter banks - A new cascade method based on window functions, *J. Fac. Eng. Archit. Gazi Univ.* <https://doi.org/10.17341/gazimmfd.473976>
- Prabhu, K.M.M. (2014). *Window Functions and Their Applications in Signal Processing*, CRC Press, Taylor & Francis Group LLC, NY.
- Sharma, I., Kumar, A. and Singh, G. (2016). Adjustable window based design of multiplier-less cosine-modulated filter bank using swarm optimization algorithms, *AEU-International Journal Of Electronics and Communications*, Vol. 70, No. 1, pp. 85-94. <https://doi.org/10.1016/j.aeue.2015.10.008>
- Sharma, S.N., Saxena, R. and Saxena, S.C. (2007). Tuning of FIR filter transition bandwidth using fractional Fourier transform, *Signal Processing*, Vol. 87, No. 12, pp. 3147-3154. <https://doi.org/10.1016/j.sigpro.2007.06.005>
- Singh, N. and Saxena, R. (2012). Development of New Combinational Window Family with its Application in the Design of Cosine Modulated Filter Bank with Better Performance, *IJECCT*.
- Singh, N. and Saxena, R. (2013). A novel window and its application in NPR type transmultiplexer design, *Electrical and Electronic Engineering*, Vol. 2, No. 6. <https://doi.org/10.5923/j.eee.20120206.01>
- Yoon, T. and Joo, E. (2010). A flexible window function for spectral analysis [DSP Tips and Tricks], *IEEE Signal Processing Magazine*, Vol. 27, No. 2, pp. 139-142. <https://doi.org/10.1109/msp.2009.935422>
- Zaytsev, G. and Khzmalyan, A. (2018). A family of optimal cosine-sum windows for real-time spectral analysis, *2018 Engineering And Telecommunication (Ent-MIPT)*. <https://doi.org/10.1109/ent-mipt.2018.00030>